

## Developments in inelastic instrumentation at ISIS

*A. D. Taylor, Z. A. Bowden, C. J. Carlile, M. E. Hagen, A. C. Hannon,  
R. S. Holt, J. Mayers, R. Osborn, M. P. Paoli, S. T. Robertson, A. Smith,  
U. Steigenberger, J. Tomkinson, and W. G. Williams*  
Rutherford Appleton Laboratory  
Chilton, Didcot, Oxon OX11 0QX  
UNITED KINGDOM

**ABSTRACT:** We summarise developments on the three scheduled inelastic spectrometers HET, TFXA and IRIS and illustrate their scientific programme with some recent highlights. We give details of commissioning experiments on PRISMA and discuss the status of the eVS and polarisation programmes. The status of the MARI project is reviewed.

### Introduction

ISIS, the world's most powerful pulsed neutron source, is now operating regularly at proton currents of 100  $\mu\text{A}$ . There has been a ten-fold increase in neutron production in the last two years, see Fig. 1. This is reflected in both the quality and quantity of the scientific programme. Of the 14 beamlines in use, see Fig. 2, nine have fully scheduled instruments with over-subscription factors varying from two to four. The inelastic instrument suite comprises three fully scheduled spectrometers (HET, TFXA and IRIS), two instruments at advanced stages of commissioning (PRISMA and eVS) and one (MARI) in the final stages of construction. This paper discusses the current state of these instruments together with the polarisation programme at ISIS.

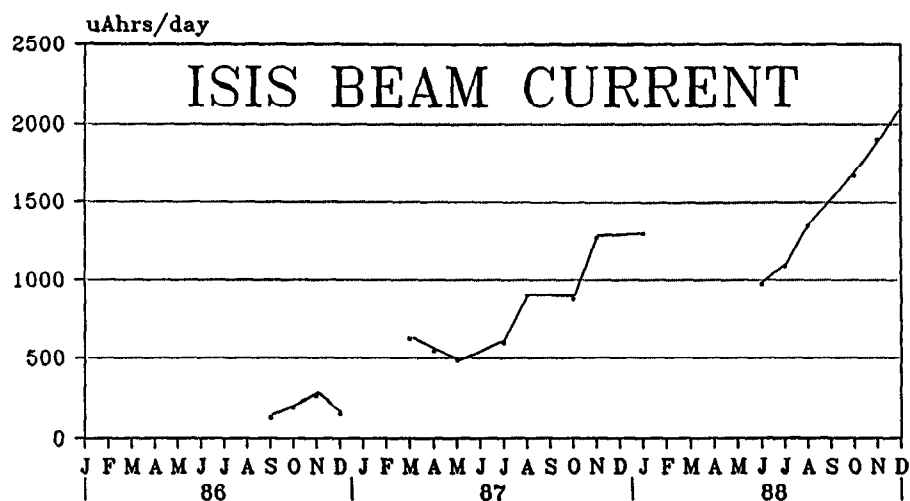


**Fig. 1** The increase in ISIS beam current over the past three years measured as a  $\mu\text{A}\cdot\text{hr}$  per day.

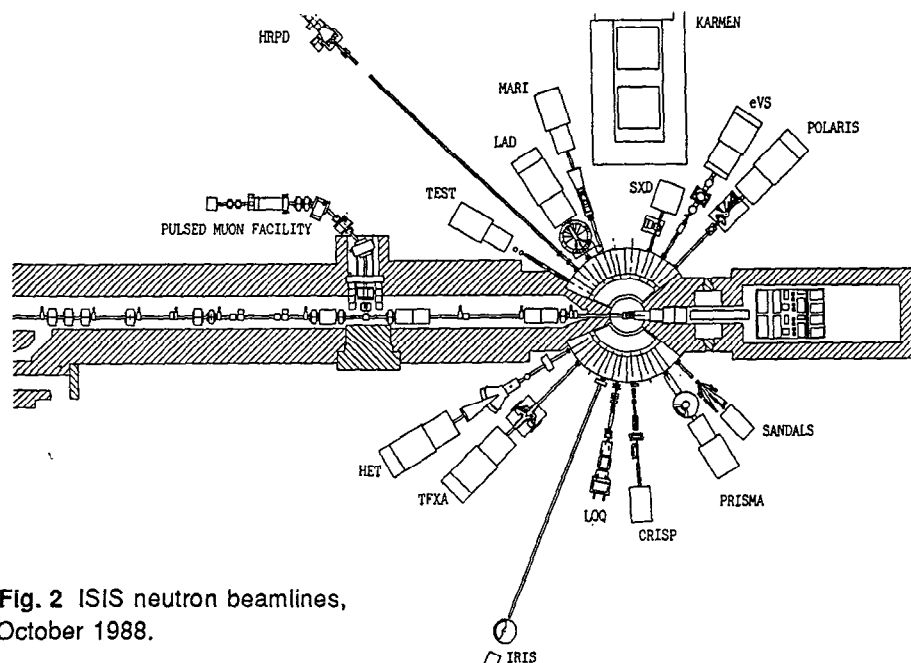


Fig. 2 ISIS neutron beamlines, October 1988.

### HET: High energy inelastic spectrometer

The HET instrument is a direct geometry chopper spectrometer designed specifically to study inelastic scattering at high energy transfer with low associated momentum transfer and good energy transfer resolution<sup>[1]</sup>. There has been a diverse scientific programme on HET with experiments on localised and itinerant magnetism, vibrational density of states, particularly of the new high  $T_c$  superconductors and momentum density measurements in model systems.

The major project on HET this year has been the upgrade of the intermediate angular range detector between  $9^\circ$  and  $29^\circ$ . The new thin window arrangement with its eight-fold azimuthal symmetry is designed to accommodate 256 high pressure  $^3\text{He}$  detectors (Fig. 3). Installation of this array involved a substantial rebuild of the secondary spectrometer during the three month long shutdown of ISIS in Spring 1988. The incident energy range of the spectrometer has been successfully extended with a new chopper slit package designed to operate at energies as low as 35 meV. All the chopper systems have been very reliable. With the substantial increase in flux from ISIS during the year, the major time loss became the pumpdown time after a sample change. This has been halved by the use of a larger turbo pump and a more efficient roughing device. Designs for a top loading cryostat with an air lock to allow "bare" samples to be changed quickly while still minimising scattering from the sample environment device are well advanced.

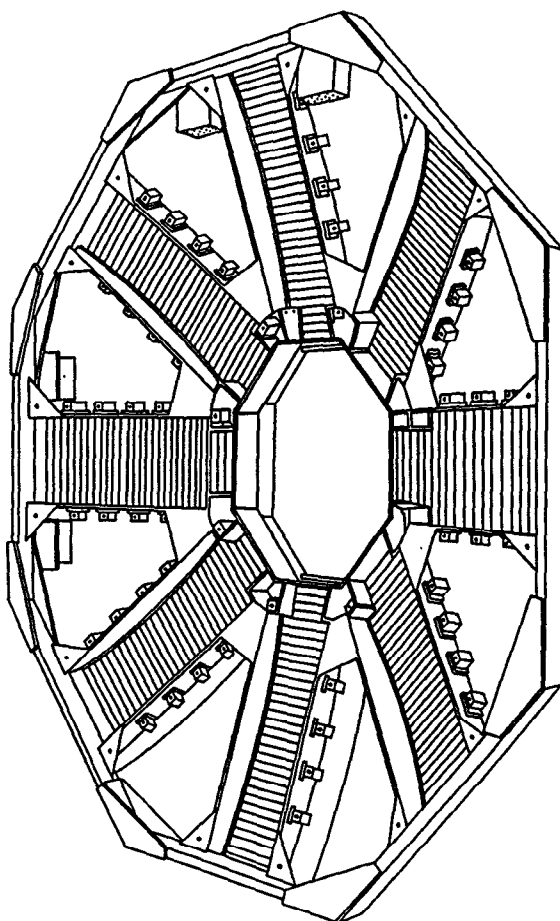


Fig. 3 The eight-fold array of 256  $^3\text{He}$  detectors, which covers the intermediate angular range on HET.

## Highlights of the scientific programme on HET

### Magnetism

The main thrust of the HET programme was in the field of magnetic scattering. The intermultiplet transition in praseodymium at 260 meV was easily observed in a specially purified sample of the metal. The Q dependence of this  $^3\text{H}_4 \rightarrow ^3\text{H}_4$  transition confirmed its magnetic origin. Such an observation was only possible because of the excellent low background of the  $^3\text{He}$  gas detectors. The same system gave a new record for high energy inelastic magnetic scattering with energy transfers in excess of 800 meV being observed<sup>[2]</sup>. The neutrons induce excitations from the ground state of the  $4f^2$  ion to excited states with different LSJ quantum numbers. Several such intermultiplet transitions were found, see Fig. 4, and this more than

---

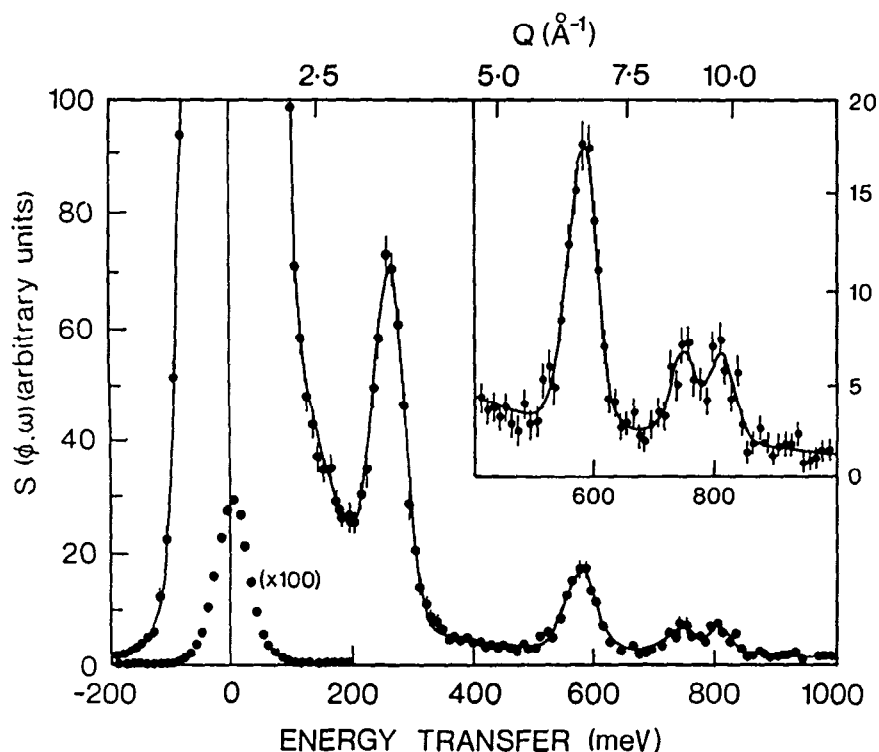


**Fig. 4** Neutron scattering cross section of praseodymium at 17 K, measured at an angle of  $5^\circ$  with an incident neutron energy of 1300 meV. The change in the scattering vector across the spectrum is shown along the top axis. The data have been fitted by four Gaussians and a tail of low energy scattering.

doubles the energy range over which magnetic excitations have been observed by inelastic neutron scattering.

The momentum transfer dependence of the intensities was found to be in good agreement with calculated, free-ion inelastic structure factors. These are not simple functions of momentum transfer, see Fig. 5. Dipole and higher order multiple excitations have been identified with the aid of these calculations. Transitions to a different value of orbital angular momentum were found to be shifted significantly from the free ion value. These results will lead to a better understanding of the interactions between localised f-electrons and delocalised conduction electrons in these rare-earth metallic systems. Again such measurements were only possible because of the excellent resolution and signal to noise achievable on a pulsed neutron source.

The high energy spin dynamics of the transition metal ferromagnets is a subject of strong current interest. A team from Cambridge University was able to measure the spin waves in cobalt to only half of their predicted maximum energy using neutrons from the hot source at the Institute Laue-Langevin (ILL). The same team have now successfully completed their measurements using a single crystal of hexagonal cobalt

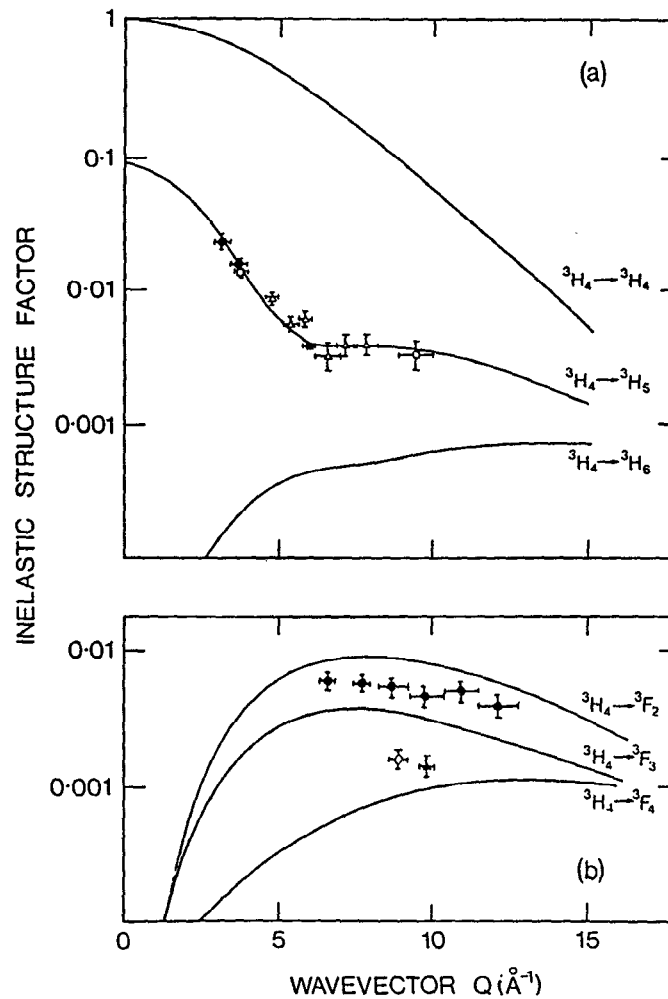


**Fig. 5** Neutron inelastic structure factors for transitions (a) within the  ${}^3\text{H}$  term, (b) from the  ${}^3\text{H}$  to the  ${}^3\text{F}$  term. The lines represent calculated intensities of the transitions. The structure factors are normalised to the  ${}^3\text{H}_4 \rightarrow {}^3\text{H}_4$  intensity at  $Q = 0$ , which has a cross section of 620 mb/sr.

on HET at ISIS, observing the spin waves to energies of up to 310 meV, see Fig. 6<sup>[3]</sup>. (It is essential to observe the full energy range of the excitations in order to distinguish between the various theoretical models). The nature of the time-of-flight scan complicates interpretation of these data somewhat, but this is more than compensated for by the good resolution and excellent signal to noise obtained by this technique, see Fig. 7. Further data analysis to extract widths and absolute intensities is in progress.

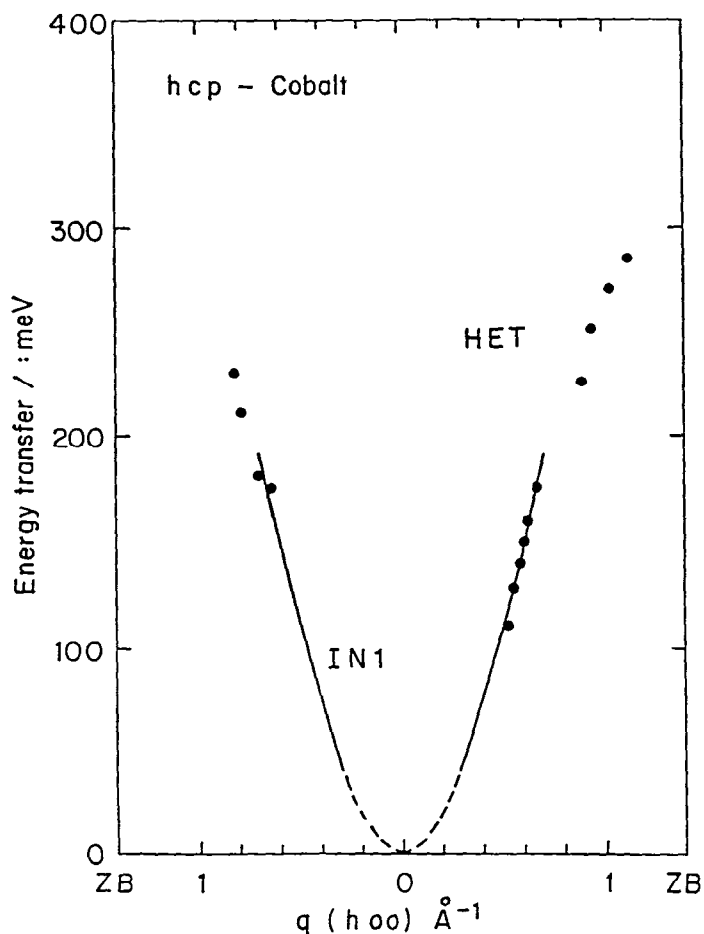
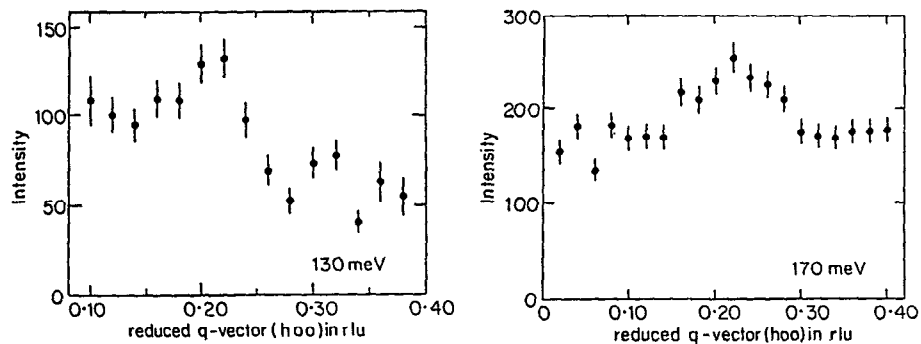
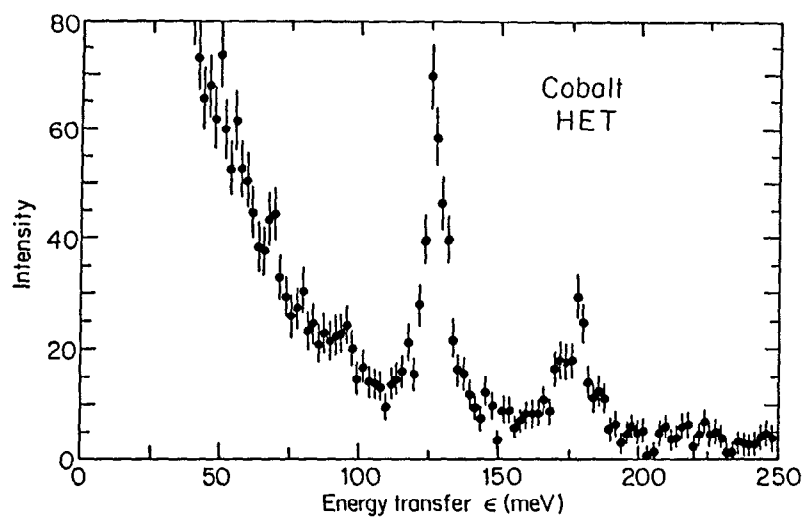


Fig. 6 The magnon dispersion relation for hcp-cobalt along the [h00] direction measured on IN1 at the ILL (line) and on HET at ISIS (dots).

Work on localised high energy magnetic excitations has continued with studies of the crystal field potential in UOS where transitions were observed up to an energy of 80 meV both above and below the antiferromagnetic ordering transition at 55 K. As in the case of  $UO_2$  both the energy and intensity of the crystal field splittings support a level scheme calculated from a point charge model<sup>[4]</sup>. In an experiment designed to refine the crystal field potential within the new ceramic superconductors<sup>[5]</sup>, the heavy rare earth ions Ho, Er and Dy were substituted for Y in the 1-2-3 compound  $YBa_2Cu_3O_{7-\delta}$ . Clearly resolved magnetic excitations were observed between 10 and 100 meV and their temperature dependence measured. The results show that the parameters of the potential can be scaled across the rare-earth series.



**Fig. 7** The 130 meV and 170 meV spin waves in hcp-cobalt measured on (a) HET and (b,c) IN1 illustrating the improved resolution and signal-to-noise obtained with the time-of-flight method.

### Vibrational spectroscopy

Work on metal hydride systems continued with a detailed study of the alpha phase  $\text{YH}_{0.11}$ . A high energy measurement, Fig. 8, illustrates the nearly harmonic behaviour of the degenerate a-b modes at 135 meV in the tetrahedral site and the extremely anharmonic behaviour of the c-axis mode at 100 meV<sup>[6]</sup>. Using a lower incident energy, a high resolution measurement revealed a splitting of this mode due to H-H pairing along the c-axis. These subtle features require a more sophisticated quantum mechanical description of the interstitial hydrogens than the perturbed simple harmonic oscillator which has until now been adequate.

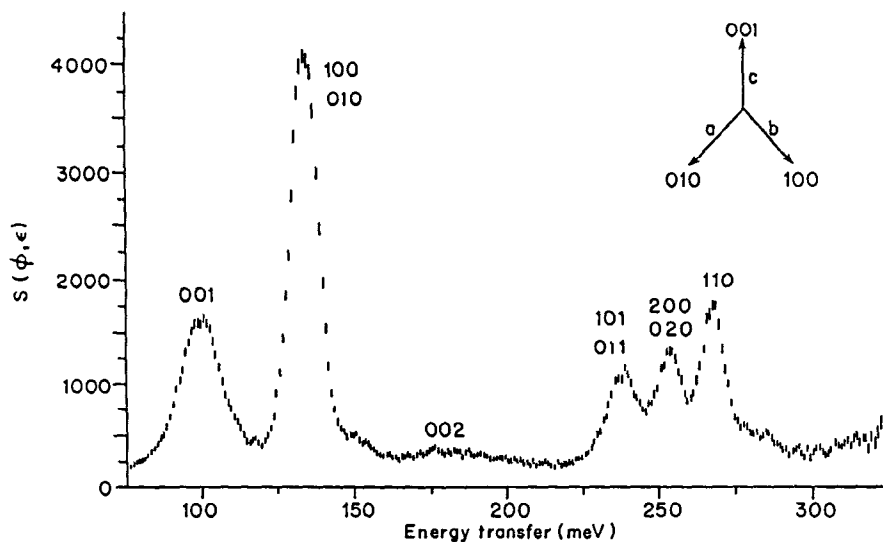


**Fig. 8** The inelastic spectrum of  $YH_{0.11}$  measured on HET with an incident energy of 330 meV. The simple harmonic quantum numbers are given for each transition.

Studies of the dynamical structure factor of amorphous boron<sup>[7]</sup> were successful despite the limited angular range of detectors available, see Fig. 9. Such problems will benefit significantly from the newly installed detector array and these results bode well for the future of such experiments on MARI.

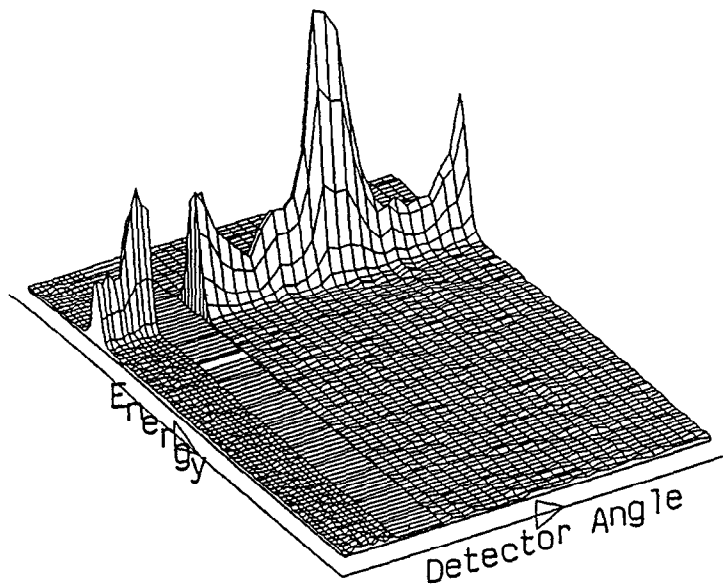


**Fig. 9** The scattering function for amorphous boron determined using an incident energy of 360 meV. The angular range covered is  $3^\circ$  to  $7^\circ$  and  $10^\circ$  to  $30^\circ$ .



### TFXA: The time-focussed crystal analyser spectrometer

TFXA is an inverted geometry neutron inelastic scattering spectrometer<sup>[8]</sup>. The sample, at 12 m from the source, is illuminated with pulses of white radiation. Neutrons lose energy by exciting vibrations in the sample, and some are scattered towards the analyser crystals. These graphite crystals are set to reflect neutrons of  $\sim 4$  meV toward the detectors. The more energetic neutrons arrive at the sample first and energy analysis is by time of flight. The spectrum was converted from neutrons per channel to  $S(Q, \epsilon)$  per energy transfer, by standard programs. The spectrometer has excellent resolution, see Fig. 10,  $\Delta\epsilon/\epsilon \leq 2\%$  and  $\Delta|Q| \sim 0.2 \text{ \AA}^{-1}$ . The fixed locus through  $Q$ - $\epsilon$  space effectively follows  $Q^2 \sim \epsilon/2 \text{ (\AA}^2\text{-meV}^{1/2}\text{)}$ .

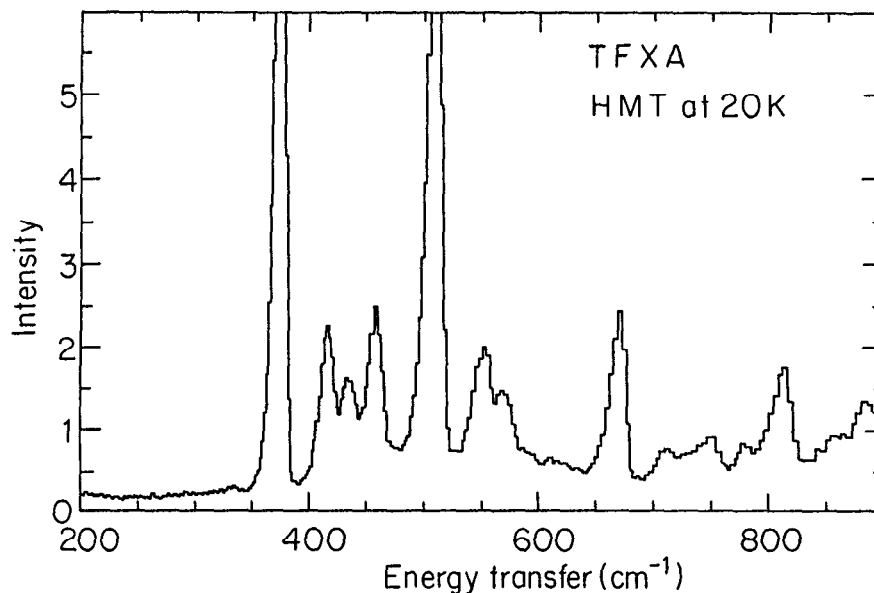


**Fig. 10** Part of the inelastic spectrum of hexamethylene tetramine (HMT) measured on TFXA. These high resolution data should be compared with the MaxEnt reconstruction given in these proceedings by D.Sivia.

Samples are held as flat plates perpendicular to the incident beam. Therefore, for energy transfers greater than  $\sim 30$  meV the momentum transfer vector  $Q$  is also perpendicular to the sample. This can be put to significant advantage in the study of some hydrogenous single crystals.

We have already reported that TFXA is almost free of the effects of multiple scattering<sup>[9]</sup>. In the case of single crystal spectra this requires some qualification. The effects of multiple scattering in single crystals is to produce spectra which are more "powder" like. Hydrogenous crystals which are ca 1 mm thick scattering ca 5% of the neutrons should not introduce significant multiple scattering problems.

## Spectrometer improvements

Since the last ICANS meeting, TFXA has seen several improvements. Principle amongst these are improvements in resolution, flux and background.

- (i) The resolution has been improved by obtaining detectors whose active thickness was matched to the secondary spectrometer. These are 6 mm thick squashed Helium tubes. At 5 bars filling pressure they are as inefficient as  $\text{BF}_3$  tubes at detecting high energy neutrons thus slightly reducing the noise.
- (ii) The count rate has been improved by obtaining thicker graphite crystals, with larger mosaic spread. There is a slight degradation in resolution attendant upon this change—but this occurs in the elastic peak region.
- (iii) The background has been improved by coating all exposed metal surfaces by cadmium. The sample is also heavily encased in cadmium. The reflection geometry of TFXA has simplified opting for this solution.

The calibration of TFXA has traditionally been based upon Hexamine (HMT) which produces a very strong inelastic line at  $\sim 390 \text{ cm}^{-1}$ , see Fig. 11. We anticipate that this choice of calibrant will have to change. This is because it produces a strong (111) Bragg reflection at the elastic energy. With our reduced elastic resolution we are no longer able to resolve the coherent and incoherent contributions to the elastic line. A systematic error introduced by this effect leads to an underestimation of the energy transfer values. This underestimate is not greater than  $4 \text{ cm}^{-1}$ .

## Data treatment

Because there are no spectral variables open to choice on the TFXA spectrometer we have instituted an automatic standard analysis program. The experimentalist automatically launches this by ending his data collection. It has the advantage of producing standard files, avoids wasting time and prevents inexperienced users from producing very badly analysed data.

Molecular spectroscopists are making good use of the CLIMAX program. This is analogous to the Rietvelt fitting programs for diffraction. Working with G. J. Kearley (ILL) we have produced a version of CLIMAX which fits phonon wings out to eighth order.

The effects of recoil scattering has also been identified on TFXA. In the context of molecular vibrations recoil is an exaggerated and smooth phonon wing. It is present when the lattice forces restricting small molecules are very weak. Useful, if limited, parameters can be extracted from the recoil spectra of simple molecules, e.g., recoil mass, average lattice energy.

## Scientific highlight on TFXA: Hydrodesulphurisation catalysts

The high sulphur content found in North Sea oils can be reduced by the hydrodesulphurisation process. The presence of sulphur poisons the surface of normal active metal catalysts in the cracking and reforming reactions necessary to

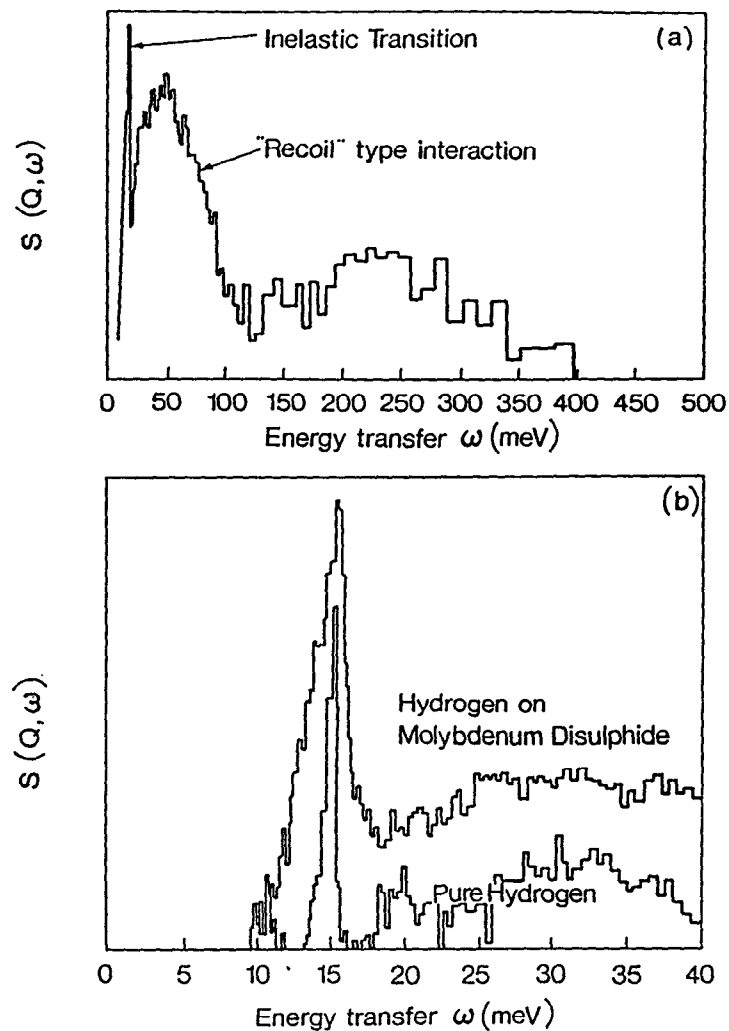


Fig. 11a TFXA data for  $H_2$  on tungsten disulphide at 50 bar.

Fig. 11b TFXA data for  $H_2$  on molybdenum disulphide at 50 bar showing the sharp  $0 \rightarrow 1$  rotational transition.

refine the oil. An understanding of the desulphurisation reaction is essential for the efficient use of expensive hydrogen.

Following earlier neutron studies on the sorption of  $H_2$  on  $MoS_2$ , work on  $H_2 + MoS_2$  and  $H_2 + WS_2$  has been extended to higher pressures<sup>[10]</sup>. The original high pressure results produced convincing evidence that more than one absorption site was present in  $MoS_2$ . The second absorption site was associated with a spectral feature at 50 meV. This site saturates at 50 bar. Kinetic data shows that the

hydrosulphurisation reaction over  $\text{MoS}_2$  is first order in hydrogen partial pressures up to 50 bar. It was assumed that the second absorption site was responsible for the behaviour of the hydrogen in this important industrial process. The 50 meV band was understood to be due to atomic hydrogen.

The TFXA data for  $\text{H}_2$  on tungsten disulphide may be compared with those obtained from solid  $\text{H}_2$  in Fig. 11. The theoretical response of a 'recoiling'  $\text{H}_2$  molecule is also shown. The TFXA results show clearly that non-dissociated  $\text{H}_2$  molecules are involved. This is confirmed by the very sharp transition at 14.7 meV which is the 0-1 rotational transition of molecular hydrogen. The spectra obtained, however, are not simply those of solid  $\text{H}_2$  condensed on the sample. This demonstration of the molecular nature of the adsorbed hydrogen as distinct from the atomic nature previously accepted has far-reaching consequences in understanding these important chemical reaction mechanisms.

### IRIS: The high resolution inelastic spectrometer

IRIS is an inverse geometry crystal analyser spectrometer optimised for high resolutions (15  $\mu\text{eV}$ ) up to moderate energy transfers (0-10 meV)<sup>(11)</sup>. It was commissioned during the second half of 1987 and is now in routine operation, although a number of major items are still being installed.

### Instrument description

The spectrometer views the ISIS liquid hydrogen cold source via a 34 m long curved neutron guide which terminates with a 2.5 m long supermirror-coated converging guide. At 6 Å the flux at the sample is enhanced by a factor of 2.8 due to the converging guide. The sample position is at 36.54 m from the moderator and the measured flux at 100  $\mu\text{Amp}$  operation of ISIS is  $5 \times 10^6$  n/cm<sup>2</sup>/sec over a sample area of 3.5 x 2.5 cm<sup>2</sup>.

At 6.4 m from the moderator a variable aperture disc chopper serves to prevent frame overlap at the detector and to eliminate ISIS pulses when a wider energy transfer range is required. At full ISIS frequency the wavelength window at the sample is 2.0 Å. The energy transfer range spanned depends upon the phase of the chopper with respect to the ISIS pulse. If the wavelength window is centred on the elastic line an energy transfer range from +0.65 meV to -0.45 meV can be observed. In downscattering only to the elastic line an energy transfer range from +1.85 meV to 0.0 meV can be observed. Decreasing the chopper speed to 25 Hz increases this measuring window to 11.1 meV. The maximum energy transfer range is limited by the short wavelength cut-off of the curved guide to a value of approximately 15 meV. At this energy transfer the resolution is  $\sim 80$   $\mu\text{eV}$  compared to 15  $\mu\text{eV}$  at the elastic line.

It is a feature of inverted geometry spectrometers that the measuring range in neutron energy loss is very large compared with a direct geometry spectrometer as a result of the opposite handedness of the (Q- $\epsilon$ ) loci, see Fig. 12. Direct geometry machines (such as IN5) achieve high resolutions by reducing the incident neutron energy such that in the limiting case a very narrow energy transfer range with only a small

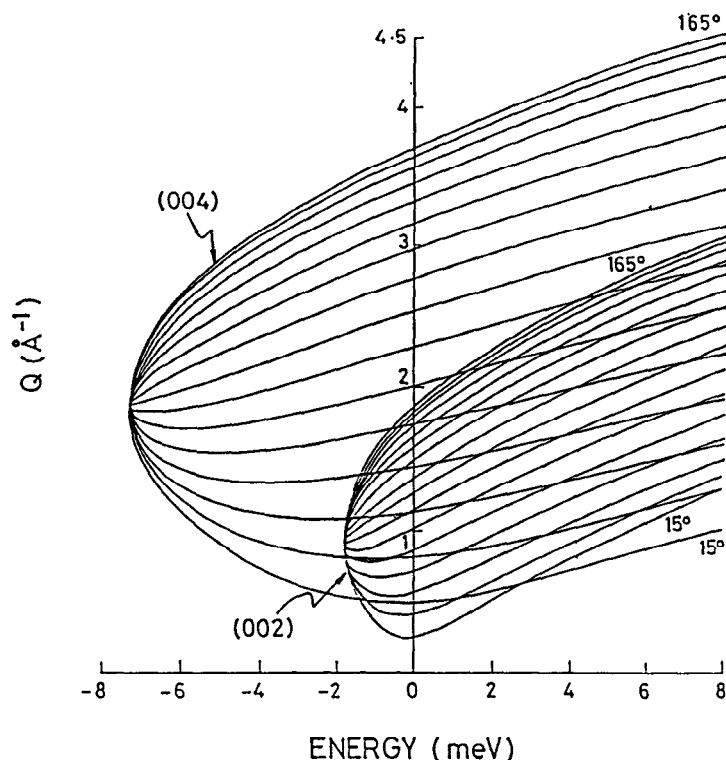


**Fig. 12** The  $Q$ - $\epsilon$  range available on IRIS from the 002 and 004 reflections of PG. The elastic resolution is  $15 \mu\text{eV}$  and  $45 \mu\text{eV}$ , respectively.

momentum transfer range is observable. Inverse geometry machines suffer from no such conflict. This feature is a great advantage when attempting to assign level schemes in tunnelling spectroscopy and crystalline electric field spectroscopy with very cold samples in their ground states.

### Planned upgrades

A new ZnS scintillator is presently being installed. This does not suffer from gamma sensitivity in the manner which the present detector does. As a result a significant contribution to the spectral background derives from the effects of neutron absorption in the sample and whilst hydrogenous sample could be studied routinely non-hydrogenous samples containing significant absorbing species proved impossible to measure. A gamma insensitive detector will also be a great relief in that we can now resort to the flexibility of shielding using cadmium!

At the same time we are installing a radial collimator between sample and analyser bank. This should reduce considerably background effects due to sample environment windows and stray neutrons, although it will also have an effect on the signal.

During 1989 we shall install a cooled beryllium filter between the sample and analyser bank. Financial constraints allow us to purchase only sufficient beryllium to cover half the analyser. This however should not be a severe restriction since it will mainly be utilised for inelastic spectroscopy where full Q coverage is not absolutely necessary initially. It will be installed to cover  $90^{\circ}$ - $165^{\circ}$  angles of scattering with the possibility of switching this to the low angle analysers for crystal field excitations if required.

### Future developments

We have tested the idea of a mica analyser with a mock-up array which was by no means optimised. An elastic resolution using the (004) mica reflection of  $5.5 \mu\text{eV}$  was recorded at an analysing energy  $833 \mu\text{eV}$ , see Fig. 13. Compare this with  $15.5 \mu\text{eV}$  presently available from the (002) pyrolytic graphite reflection analysing at  $1.835 \text{ meV}$  with a count rate  $\sim 25 \times$  higher. Despite this reduction in counting times, it was possible to observe tunnelling peaks at  $\pm 15 \mu\text{eV}$  and  $+150 \mu\text{eV}$  in 4-methyl pyridine zinc chloride, never previously observed, in a 16 hour run. We believe the  $15 \mu\text{eV}$  peaks are the lowest energy transfers observed to date at a pulsed neutron source. Theoretically it is possible to use the (002) mica reflection to obtain resolutions of the order 1 to  $2 \mu\text{eV}$  at an analysing energy of  $208 \mu\text{eV}$  but we were not able to observe the elastic line due to frame overlap problems. (The (002) reflection is detected on IRIS 10 pulses after the neutrons left the moderator!). This may seem an impossible goal but we are planning to build a large area mica analyser (at least 10 times larger than the prototype) focusing onto a single detector for use in inelastic spectroscopy for operation in late 1989. We also plan to investigate methods of increasing the mica reflectivity. The 4-MPZnCl<sub>2</sub> could then be collected in 1 1/2 hours (or 45 minutes at 200  $\mu\text{Amps}$ ) and the transition to the mica (002) reflection with its 1-2  $\mu\text{eV}$  resolution is becoming attainable. (It should be remembered that run times on IN10 are typically 24 hours.)

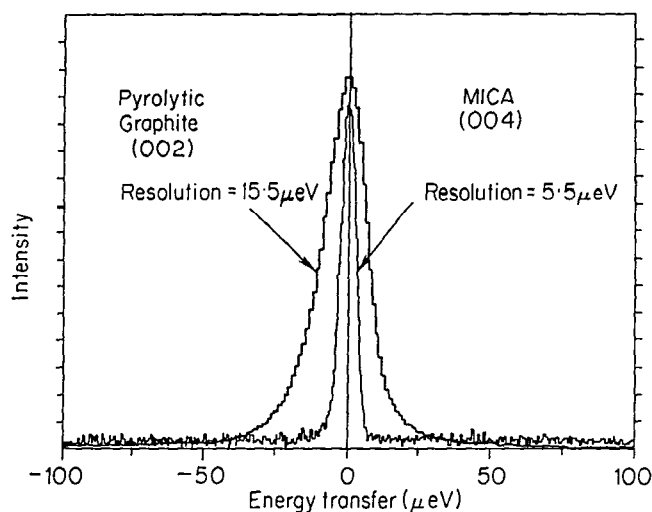


**Fig. 13** Test data on IRIS comparing the  $5.5\text{-}\mu\text{eV}$  resolution available from Mica (004) with the standard  $15\text{-}\mu\text{eV}$  resolution of PG (002).

### Scientific highlight on IRIS: Intermolecular coupling in 4-methyl-pyridine

$C_5NH_4 \cdot CH_3$  have been revealed by neutron scattering on the IRIS spectrometer. The tunnel level in 4-methyl-pyridine at 520  $\mu\text{eV}$ , very close to the free rotor limit for a methyl group of 665  $\mu\text{eV}$ , is one of the few examples of an almost-free rotor found in the solid state. Instead of a single tunnel level expected from a molecule which is non-interacting with its surroundings, the tunnel spectra of 4-methyl-pyridine measured on IRIS exhibits four discrete components centred around 520  $\mu\text{eV}$ , see Fig. 14. In an attempt to unravel the cause of the complex spectrum, a series of experiments have been performed on IRIS varying both temperature and the dilution of the hydrogenated molecules with fully deuterated molecules. Both increased temperature and increased dilution clearly weaken the coupling between neighbouring molecules giving rise to an anomalous rise in the tunnelling frequency as a function of temperature at low concentrations. The results are being modelled theoretically using the concepts of dynamic and static coupling of methyl groups employing gauge theory<sup>[12]</sup> and by utilising the sine-Gordon formalism which proposes the existence of soliton-antisoliton waves<sup>[13]</sup>.

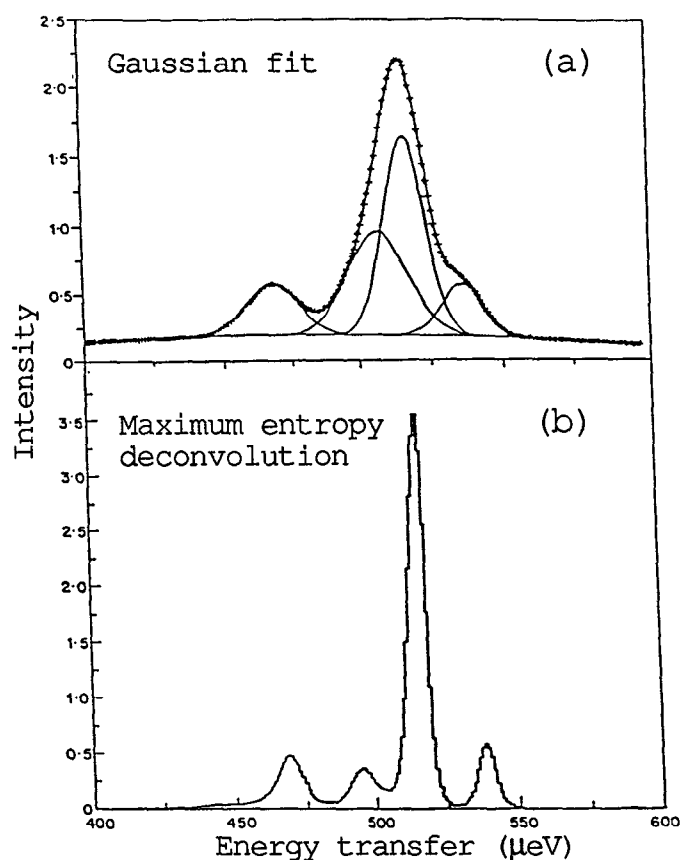


Fig. 14 Decomposition of the 520 meV tunnel level in 4-methyl-pyridine into four components (a) by Gaussian fitting and (b) by the maximum entropy method.

## PRISMA:

### A high-symmetry inelastic spectrometer

PRISMA stands for **PR**ogetto dell'Istituto di Struttura della **MA**teria del CNR. Under an international collaboration signed in 1985 between SERC and the Consiglio Nazionale delle Ricerche, CNR, Frascati, Italy, PRISMA has been provided by Italy for installation on ISIS.

PRISMA is designed to measure coherent excitations in single crystals<sup>[14]</sup>. The scattering function  $S(\mathbf{Q},\epsilon)$  is measured along a high-symmetry direction in reciprocal space to be determined by the experimentalist. With the present set of germanium analysers the energy transfer range reaches up to 200 meV (depending on the choice of wavevector  $\mathbf{Q}$ ).

The instrument operates in inverted geometry, i.e., it has a white incident neutron beam. The energy change of the scattered neutrons is analysed by 16 independent analysers, each equipped with a detector. The angular separation between the individual detectors is  $2^\circ$ , so a total  $\phi$ -range of  $30^\circ$  is covered, see Fig. 15. Keeping the ratio  $(\sin\phi_i/\sin\Theta_{A_i})$  constant for all analysers ensures that every analyser-detector arm records  $S(\mathbf{Q},\epsilon)$  along the same  $\mathbf{Q}$ -direction in reciprocal space. The positioning of all analyser and detector motors, as well as of the motors for the sample angles  $\phi$  and  $\Psi$  and the sample goniometer, are controlled by a dedicated PC.

An elaborate software package has been developed for communication between the PRISMA control programme, the standard ISIS data acquisition, CAMAC software and the IBM personal computer which controls the 34 positioning motors (16 analysers, 16 detectors, the rotating collimator and the  $\phi$ -arm). This allows to set up the spectrometer by computer in every desired configuration. Also a single motor or a physical quantity (like the analysing energy of an analyser) can be driven and scanned individually. A simulation program including a graphics display enables the experimentator to select in advance the most favourable configuration for an experiment.

Within the past few weeks, commissioning experiments have yielded very promising data, demonstrating clearly the power of this instrument to measure dispersion curves. As an example we show the phonon dispersions along the  $[1,0,0]$  direction of a single crystal of copper. Figure 16 summarises the results from all the available detectors. The curved solid lines indicate the time-of-flight loci of the 16 detectors, with the thick line marking the detector whose spectrum is shown in Fig. 17. The measurements were performed at room temperature and therefore phonons in energy gain and energy loss were observed. We would like to stress that this dispersion curve was the result of a single setting of the instrument. The data were obtained in 1.6 mA-hr, equivalent to less than a day running at current ISIS conditions. It is also evident from Fig. 17 that instrumental resolution effects influence strongly the shape of the spectra. Therefore a powerful software programme is required and is at present under development, in order to analyse the data in an appropriate way.



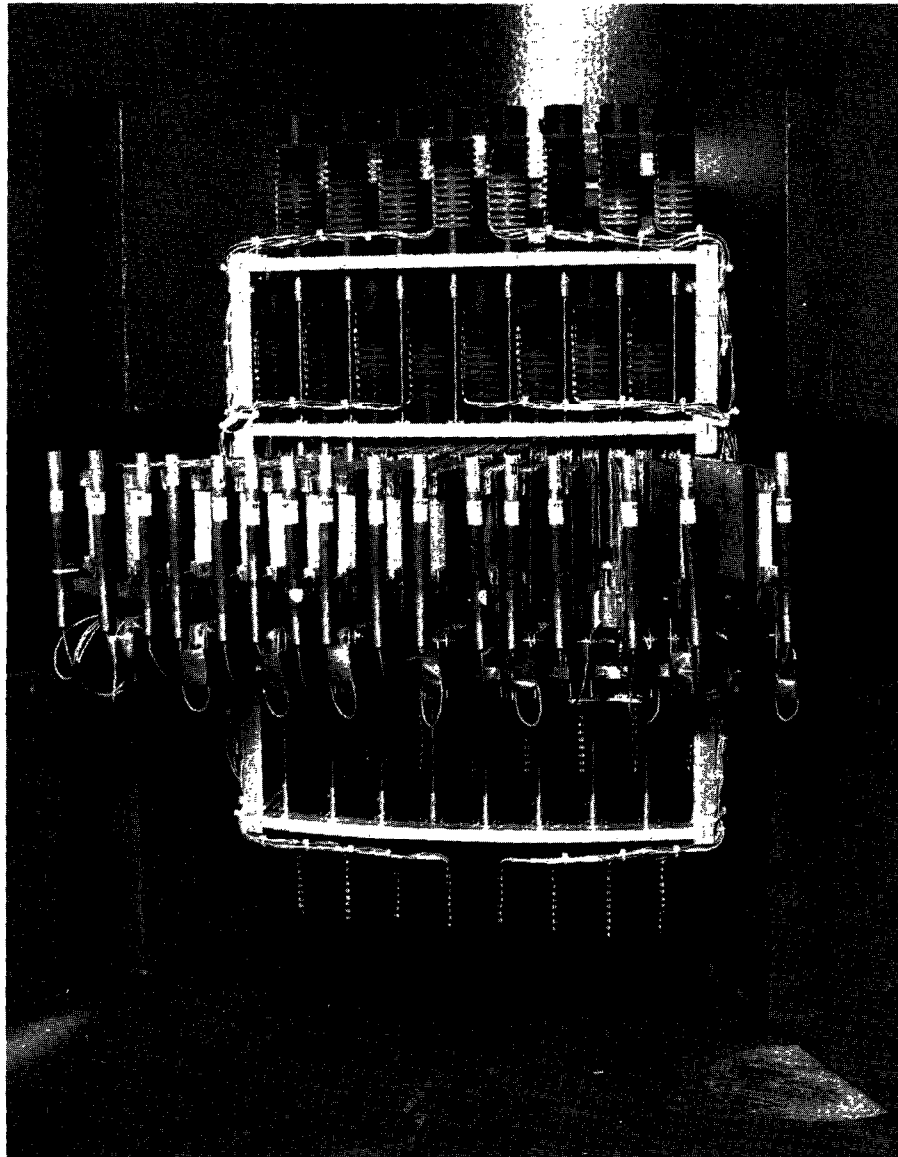


**Fig. 15** The PRISMA spectrometer with part of the shielding removed to show the  $\phi$ -arm with the 16 analyser-detector arms and the pathway of the  $\phi$ -arm through the shielding.

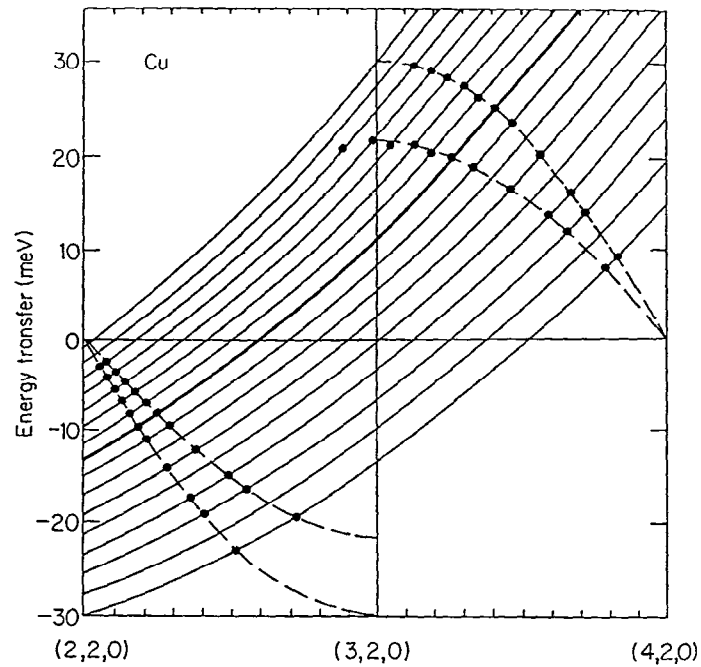


**Fig. 16** The phonon dispersion relation measured along the [100] direction in a single crystal of copper during early tests on PRISMA. The solid lines are the loci in  $(\mathbf{Q}, \varepsilon)$  space scanned by each detector, while the dashed lines indicate the known dispersion relation. The locus corresponding to detector no. 9 is highlighted.

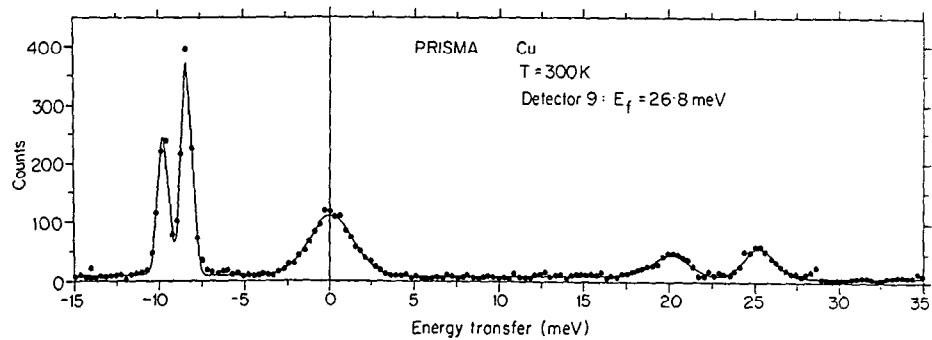


**Fig. 17** The spectrum of one individual detector (no. 9). Phonons in both energy gain and loss are clearly seen.

**eVS: The electron volt spectrometer**

**Low-Q programme**

The original goal of eVS was to explore high energy transfer scattering at low values of associated momentum transfer using  $(n,\gamma)$  detectors<sup>[15]</sup>. A review held in Spring 1988 concluded that below 500 meV transfer, chopper spectrometers such as HET had significantly better resolution and count rate than was achievable by this method. (Figure 18 compares the observation of intermultiplet transitions in praseodymium on HET and eVS). Above 1000 meV transfer this conclusion would be reversed, but the interesting cross-sections such as those associated with interband electronic excitations are predicted to be far too small to be observable with current instrumentation. As a result of this review the high energy transfer, low Q programme on eVS has been terminated.

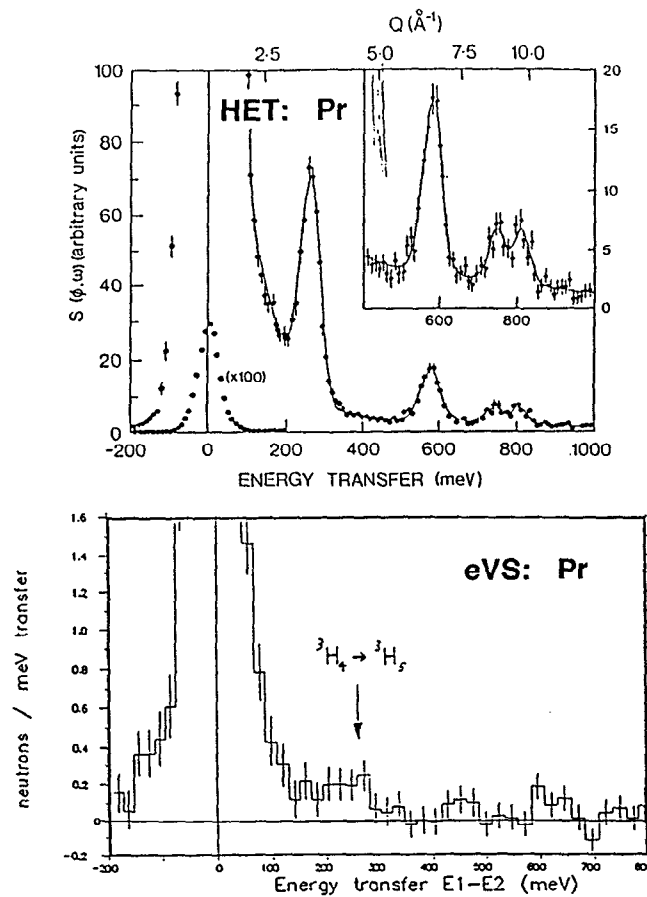


**Fig. 18** Intermultiplet transitions in metallic Pr observed in 1300  $\mu\text{A-hr}$  on HET (top) and in 7000  $\mu\text{A-hr}$  on eVS (bottom).

### High-Q programme

Progress on the high Q programme of eVS has continued with the development of a multidetector system based on the  $(n,\gamma)$  capture resonance in thin foils. An array of seven Bismuth Germanate (BGO) photon detectors was installed and commissioned using Ta annular analysing foils ( $E_f = 4.28$  eV, 10.3 eV and 23.9 eV) with a range of thicknesses between 10  $\mu\text{m}$  and 50  $\mu\text{m}$ . Measurements have been undertaken at high energy and momentum transfers which allows the momentum density of the recoiling atoms to be obtained within the impulse approximation. Several experiments within this regime have been carried out on polycrystalline graphite and a comparison between the single and multidetector systems made in terms of the signal count rates and signal to noise. The signal count rate is 20 times greater for the multidetector system albeit with a small loss in overall signal to background compared to a single detector system. In further measurements on polycrystalline Be the counting statistics were sufficient to allow data to be analysed using all three main resonances in Ta. Figure 19 shows the recoil scattering spectra from Be and the Al sample container on an energy transfer scale using the 4.28 eV resonance. Also shown is a two-Gaussian fit to the data. Measurements undertaken at 16 K on the same sample have clearly indicated the corresponding decrease in the mean atomic kinetic energy (extracted from the recoil width) in agreement with theoretical models based on the phonon density of states. Recent data have been analysed using the method of  $\gamma$ -scaling where it has been possible to compare directly recoil scattering data obtained on both eVS and HET.

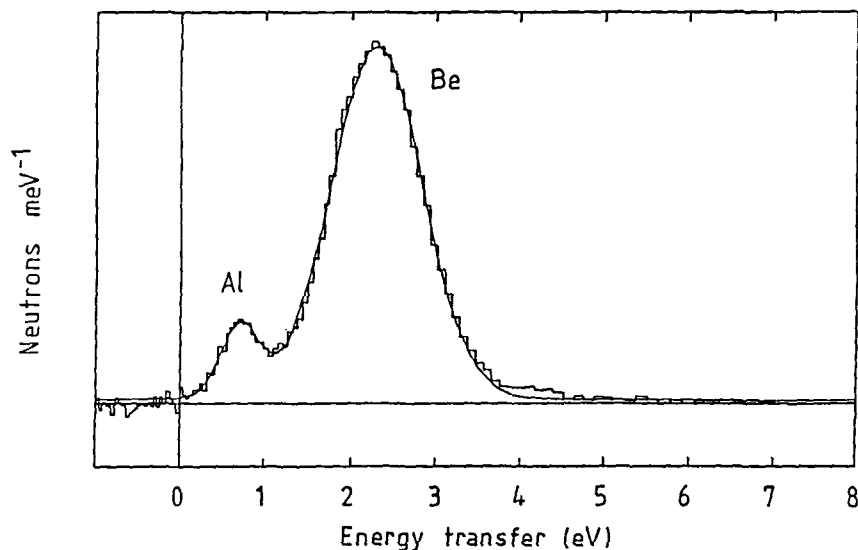


**Fig. 19** The recoil spectrum from polycrystalline beryllium obtained on eVS with the 4.28 eV resonance in Ta.

Due to an increase in the demand for studies of momentum distributions on ISIS the present eVS system has been modified and extended to undertake recoil scattering from hydrogenous materials. The fixed high-angle system imposes kinematical constraints which does not allow recoil scattering from mass 1 particles. An intermediate angle recoil spectrometer has therefore been developed to cover the angular range  $30^\circ$ - $120^\circ$  using  $30 \text{ He}^3$  detectors positioned  $0.5 \text{ m}$  away from the sample. Figure 20 shows the new eVS spectrometer on ISIS. Curved analyser foils of Ta and Au are available providing a range of energy and momentum transfers. The resonance filter difference method will be used to obtain the recoil scattering spectra. Preliminary trial measurements on  $\text{ZrH}_2$  with Ta and Au have produced some promising results in terms of both signal count count and signal to noise. A user programme for the study of hydrogenous samples is already scheduled on this spectrometer.

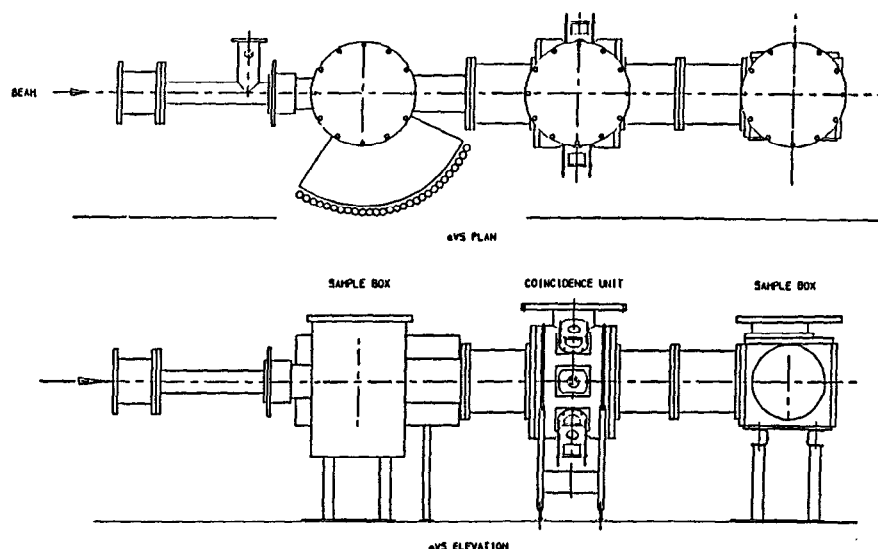


**Fig. 20** The intermediate angle spectrometer on eVS, which is optimised for recoil scattering from mass 1 and mass 2 systems. Energy analysis is performed using tantalum or gold resonance difference techniques.

### Future developments

In an attempt to return to the original goals of the eVS programme, namely the study of high energy excitations at low values of associated momentum transfer, a new spectrometer design is being investigated. Drawing on experience from HET, it would be a high resolution direct geometry spectrometer which would cater to the existing demand for high resolution magnetic scattering and would allow Brillouin scattering in amorphous systems to be explored, see Fig. 21. In addition a parallel development programme on high energy monochromating choppers and tests on polarised beams on chopper spectrometers could be performed. Detailed studies of the feasibility of constructing such a spectrometer at modest cost utilising existing

equipment are in progress. Sources of external funding for this project are also being explored.

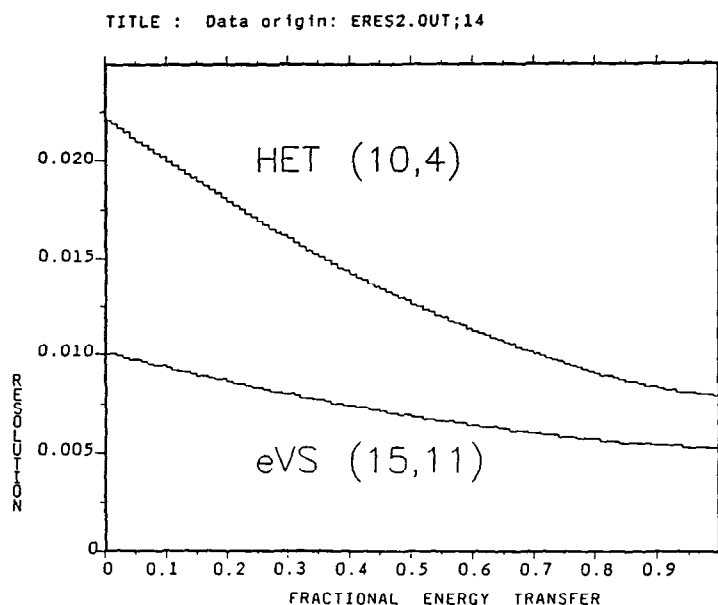


Fig. 21 The energy transfer resolution ( $\Delta\epsilon/E_i$ ) of the proposed high resolution spectrometer (Primary flight path 15 m, Secondary flight path 11 m) as a function of fractional energy transfer ( $\epsilon/E_i$ ) compared with HET.

### MARI: The multi-angle rotor instrument

The MARI project, a joint collaborative venture between RAL and the Japanese National Laboratory of High Energy Physics (KEK), is now under construction at the ISIS facility. The instrument is based on a fast Fermi chopper device, similar to that used on HET, providing energy transfer resolutions,  $\Delta E_i/E_i \sim 1\%$ . The chopper system, manufactured by Uranit GmbH at Julich, was recently delivered to RAL. An identical chopper system and associated rotor package has been manufactured for KEK. The spectrometer will view the 100 K liquid methane moderator and will use incident energies in the range 50-1000 meV. A unique feature of this new spectrometer will be that it will record inelastic scattering processes in the vertical plane using a large angular array of helium detectors with a coverage between  $\pm 10^\circ$  and  $10^\circ$ - $135^\circ$  (see Fig. 22). This will provide an accurate interpolation from  $S(\phi, t)$  to  $S(Q, \epsilon)$ . The low angle octagonal bank and the large detector vessel, containing three  $^3\text{He}$  detectors at each angle, forms a continuous angular coverage and is well shielded internally with  $\text{B}_4\text{C}$  plates and collimation vanes. This large angular range together with the high resolution will enable science to be undertaken in areas such as molecular spectroscopy, magnetic excitations, measurements of  $S(Q, \epsilon)$  and momentum distributions. It is anticipated that commissioning experiments will begin in the spring of 1990.

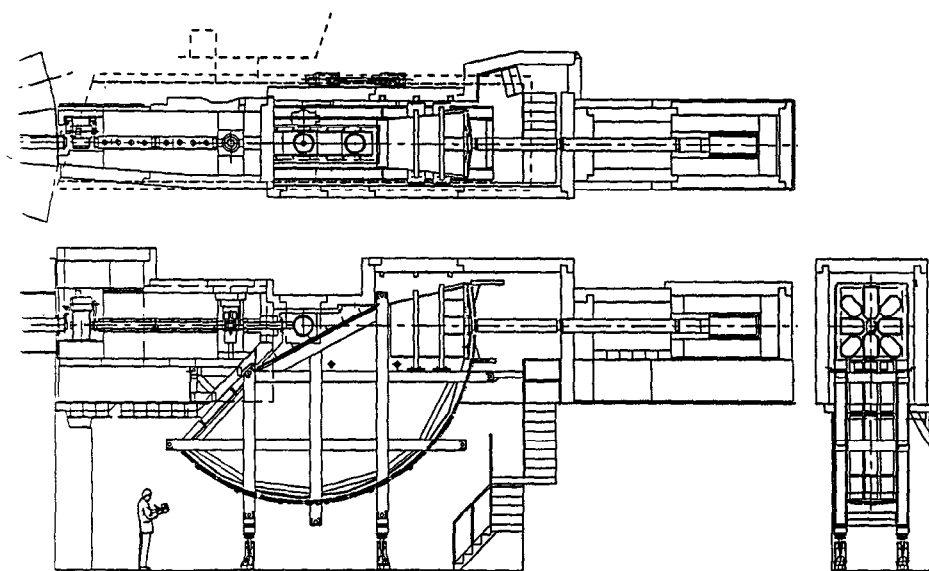


Fig. 22 Plan and elevation views of the MARI spectrometer.

### The polarisation programme at ISIS

A series of measurements made in 1985-86 on a sintered  $\text{SmCo}_5$  filter showed that this material has very good intrinsic properties as a neutron polariser at all neutron energies up to about 160 meV. The polarising efficiency in this energy range varied between 98% and 70% with corresponding transmittances between 10% and 30%. These results were obtained at approximately 1% of the ISIS design current ( $\sim 2 \mu\text{A}$ ).

Later measurements at 10% of the full ISIS current showed significant filter heating effects. The polarising efficiency at the  $^{149}\text{Sm}$  resonance peak energy (97 meV) was reduced to 65% and the transmittance to 3%. This corresponds to a nuclear spin temperature in the filter of  $\sim 70$  mK, whereas an independent measurement of the dilution refrigerator temperature by Co nuclear orientation thermometry gave 13 mK. Subsequent tests showed that this heating was caused by poor thermal contact between the filter material and the mixing chamber of the dilution refrigerator.

Considerable effort was put into achieving a good metal-metal contact between the filter material and the copper filter holder. A successful solution to this problem was found first by ion implanting copper on to the surface of the filter, and then soldering this to a copper plate which formed part of the mixing chamber base. A filter prepared in this way was found to be well-coupled to the mixing chamber and the limiting factor determining the performance of the filter was then found to be the cooling power of the refrigerator. Two observations supported this deduction: (i) the filter temperatures measured by neutrons was equal to the mixing chamber temperature measured by Co nuclear orientation, and (ii) the time constant for cooling the filter was longer than in previous filters, and equal to the cooling time of

the fridge. The cooling power of the dilution refrigerator used in this test was  $\sim 1$   $\mu$ watt at 20 mK (the temperature required for an effective filter performance), and from this it was concluded that a 40  $\mu$ watt dilution refrigerator (which is now commercially available) is required for effective filter operation in the incident beam on the Polaris beam with ISIS operating at 100  $\mu$ A.

This development programme has been discontinued for the present. Although only partially successful we can conclude that: (i) it is feasible to construct a large area polarisation analyser using the permanent magnetic material  $\text{SmCo}_5$  for neutron energies  $E < 200$  meV (the advantages of not requiring an applied field are self evident) and (ii) the method can also be used in the primary beam on a pulsed source chopper monochromator, since monochromatic fluxes would not be sufficient to heat the filter.

The current plans for polarisation work at ISIS are to construct a polarising bender made from Co/Ti supermirrors with Gd/Ti antireflecting layers. The device designed has a length  $\sim 1.2$  m with a critical wavelength  $\lambda^* \sim 0.87 \text{ \AA}$  ( $E^* \sim 110$  meV) and is similar in design to the bender on the LOQ spectrometer. It is expected to be available for first tests towards the end of 1989.

### Acknowledgements

We would like to thank the engineers, physicists and operations crews of ISIS and our technical support staff for their hard work and dedication.

### References

- [1] A D Taylor, B C Boland, Z A Bowden and T J L Jones, Rutherford Appleton Laboratory Report RAL-87-012 (1987)
- [2] A D Taylor, R Osborn, K A McEwen, W G Stirling, Z A Bowden, W G Williams, E Balcar and S W Lovesey, *Phys Rev Lett* **61**, (1988) 1309-1312
- [3] T G Perring and G L Squires, ISIS Experimental Report RB/140, p A119 in 'ISIS 88' RAL-88-050
- [4] G Amoretti, A Blaise, J M Fournier, R Caciuffo, J Larroque, R Osborn, A D Taylor and Z A Bowden, *J Magnetism and Magnetic Materials* **77/78** (1988)
- [5] B D Rainford, D McK Paul, S Culverhouse and R Osborn, ISIS Experimental Report RB/414, p A114 in 'ISIS 88' RAL-88-050
- [6] S M Bennington, D K Ross, M J Benham, A D Taylor and Z A Bowden, *Z Physik* 1989 (in press)
- [7] U Dahlborg, R G Delaplane and A C Hannon, ISIS Experimental Report RB/250, p A111 in 'ISIS 88' RAL-88-050
- [8] J Penfold and J Tomkinson, Rutherford Laboratory Report RAL-86-019 (1986)
- [9] P S Goyal, J Penfold and J Tomkinson, Rutherford Laboratory Report RAL-86-070 (1986)
- [10] P N Jones, E Knozinger, W Langel, R B Moyes and J Tomkinson, *Surface Sc* **207** (1988) 159
- [11] C J Carlile, *Nucl Inst and Meth* (in preparation) 1989
- [12] C J Carlile, S Clough, A J Horsewill and A Smith, submitted to *Chemical Physics* 1989



- [13] F Fillaux and C J Carlile (in preparation) 1989
  - [14] C Andreani, C J Carlile, F Cilloco, C Petrillo, F Sacchetti, G C Stirling and C G Windsor, Nucl Inst and Meth A254,(1987) 333.
  - [15] M P Paoli, D Phil Thesis, Oxford University 1988
-